




Minimizing satellite residence time in the GEO region through elevated eccentricity method

İbrahim Öz *¹ 

¹ Ankara Yıldırım Beyazıt University, Technology Transfer Office, Türkiye, ibrahim11oz@gmail.com

Cite this study: Öz, İ. (2024). Minimizing satellite residence time in the GEO region through elevated eccentricity method. Turkish Journal of Engineering, 8 (3), 416-426

<https://doi.org/10.31127/tuje.1395250>

Keywords

Geostationary orbit
Space debris
Graveyard orbits
Remove retired satellites
Geostationary protected region

Research Article

Received: 23.11.2023
Revised: 29.02.2024
Accepted: 01.03.2024
Published: 05.07.2024



Abstract

This research focuses on a critical aspect of the space environment, addressing the escalating issue of space debris and congestion in the geostationary orbit. The geostationary orbit is facing many satellites, leading to hazardous congestion levels and jeopardizing the limited resources available. Although organizations have established regulations for retiring satellites to graveyard orbits, a complete removal is not always achievable for numerous reasons. In response to this challenge, our study proposes a practical and cost-effective solution to mitigate debris accumulation in the region. In addition to the above, our research focuses on protecting the geostationary space environment, especially in unforeseen events involving inclined-operated satellites. We explore the implementation of an elevated eccentricity method, increasing the eccentricity of aging satellites and assessing its impact on their time in the geostationary and geostationary-protected regions. Our analysis encompasses short-term, medium-term, and long-term periods, enabling us to evaluate the effectiveness of this approach over different time frames. The study reveals a significant reduction in the time satellites spend in these regions as their eccentricity increases. Moderate eccentricity levels can reduce satellite residence time in these regions from 100.00% to 3.81%. This compelling evidence demonstrates the feasibility and effectiveness of adopting elevated eccentricity as a viable strategy to mitigate space debris in the regions. This proposed approach offers satellite operators a reliable and cost-effective solution, ensuring safe operations and protecting critical regions for aging GEO satellites. Accordingly, we contribute to space environment protection, securing the sustainability of the geostationary orbit.

1. Introduction

Space is expansive and infinite, and now, it is utilized to host satellites that are essential for modern communication, navigation, earth observation, and scientific research. The geostationary region is a critical zone within this domain, accommodating a cluster of satellites in geosynchronous orbits. However, this coveted geostationary orbit is encountering unprecedented challenges. The rapid spread of satellites, coupled with aging spacecraft and debris fragments, has led to an alarming rise in overcrowding, posing a substantial threat to the sustainability and safety of this orbital zone. Protecting the geostationary region ensures continued access to this valuable resource. Space debris, a collective term for defunct satellites, spent rocket stages, and fragments resulting from collisions or breakup, disseminates a hazardous environment. The escalating accumulation of debris amplifies the risk of collisions, creating a cascading effect that generates more fragments and endangers operational satellites. In

response to these challenges, the scientific community and space industry have embarked on a quest to safeguard the geostationary region and mitigate the space debris hazard. Various innovative approaches, including advanced tracking and monitoring systems, collision avoidance maneuvers, and novel strategies, have emerged as potential solutions to ease congestion and protect satellites operating within this region.

Geostationary orbit (GEO, also known as geosynchronous orbit) is a region of space approximately 35786 km above the Earth's equator used by many artificial satellites, including communications satellites, weather satellites, and military satellites. However, the geostationary orbit can become congested with debris over time, posing a risk to operational satellites and creating additional challenges for satellite operators.

GEO-orbital debris mitigation reduces the amount of debris in geostationary orbit and minimizes the risk of collisions with operational satellites. Several strategies can be used to mitigate geo-orbital debris, including removing debris from orbit: several organizations, such

as the European Space Agency (ESA) and the Japan Aerospace Exploration Agency (JAXA), are working on technologies and techniques to remove debris from orbit.

The Inter-Agency Space Debris Coordination Committee (IADC) is an international organization that promotes cooperation and coordination among space agencies and organizations to address the issue of space debris. The IADC has developed several recommendations for satellite operators to follow when planning the end of life of satellites to minimize the generation of additional space debris. This includes conducting maneuvers to deorbit the satellite at the end of its mission or placing it into a graveyard orbit where it will not interfere with other objects in space [1]. These recommendations aim to reduce the amount of space debris generated and to ensure the long-term sustainability of geostationary orbit.

The IADC defines the GEO-protected region as the volume of space between 200 km below the GEO altitude (35786 km) to 200 km above the GEO altitude, extending

15° on either side of the equator as shown in Figure 1a and Figure 1b. This region was designed to include a nominal operational altitude excursion of GEO ± 75km and an additional 125 km on either side for a satellite translational corridor [2].

This scientific exploration aims to investigate the complexities of space environment protection, focusing on preserving the integrity and functionality of the geostationary orbit. This study aims to assess the efficacy of the elevated eccentricity method, analyze its impact on debris mitigation, and propose sustainable strategies to ensure the long-term viability of the geostationary region. Through meticulous research and data-driven analysis, this investigation aims to contribute to the collective effort to safeguard the geostationary orbit, fostering a secure and sustainable environment for current and future space missions. Ultimately, the goal is to fortify our capacity to explore, communicate, and innovate while upholding the integrity of the space environment.

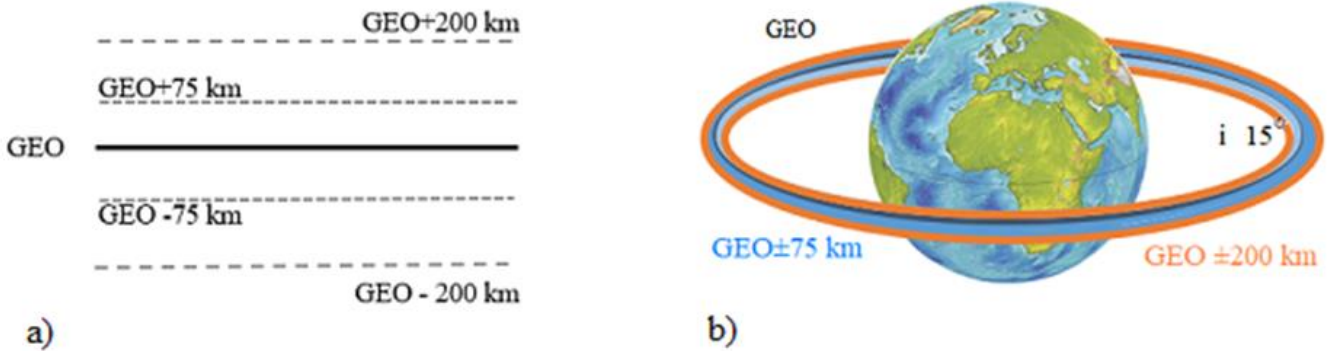


Figure 1. Illustration of geosynchronous orbit and geo-protected region a) two-dimensional b) 3D view (not to scale).

1.1. GEO orbit population

Determining the exact number of satellites in geostationary orbit at any given time is challenging, as the number can fluctuate due to factors such as launches, decommissioning, and others. However, according to data from Celestrak, as of December 2022, there were around 837 satellites in geostationary orbit, out of which 352 were active, as shown in Figure 2a. Figure 2b illustrates the satellite distribution histogram based on inclination and the orbital altitudes, that is, inclination less than 15° and in the geostationary protected region (GEO± 200km).

Figure 2c presents the histogram of 446 inclined satellites in the geostationary-protected region (1°<inclination<15° and altitude GEO±75 km). Active satellites are used for various purposes, including communications, weather forecasting, and military operations.

It is found that a significant number of GEO satellites (485 out of 837) have inclinations greater than 1 ° and that this trend has been increasing in recent years, with new classes of GEO networks being deployed with high inclinations and low to moderate eccentricities. This increase in the use of higher inclinations for GEO spacecraft leads to an increase in the number of objects in the GEO region. The number of increased objects in the

GEO region highlights the importance of properly retiring satellites to minimize the risk of space debris [3].

1.2. GEO inclined orbit and satellite failure

Satellite operators operate the aging satellite, which is close to running out of fuel to extend its maneuver life. The maneuvers consume different amounts of propellant, with the north-south station-keeping consuming more. In order to extend the lifetime of a communication satellite, operators may choose to stop performing the more fuel-intensive north-south station-keeping maneuvers and operate the satellite in an inclined orbit, known as an inclined geosynchronous orbit. All ground stations do not track these orbits but can provide special services to those with tracking capability [4,5]. A satellite's working life refers to the time a satellite can function effectively in orbit before it needs to be replaced or decommissioned. Operators generally prefer satellites with longer working lives, but this cannot be achieved easily due to various factors, such as the complexity of the satellite's subsystems.

Furthermore, it's crucial to note that launcher performance also plays a significant role in determining the maneuver life of a satellite. Extending the design life typically results in heightened mass and higher development costs, demanding additional subsystem

requirements. This delicate balance between design life, cost, and mass remains a pivotal consideration in satellite design and development.

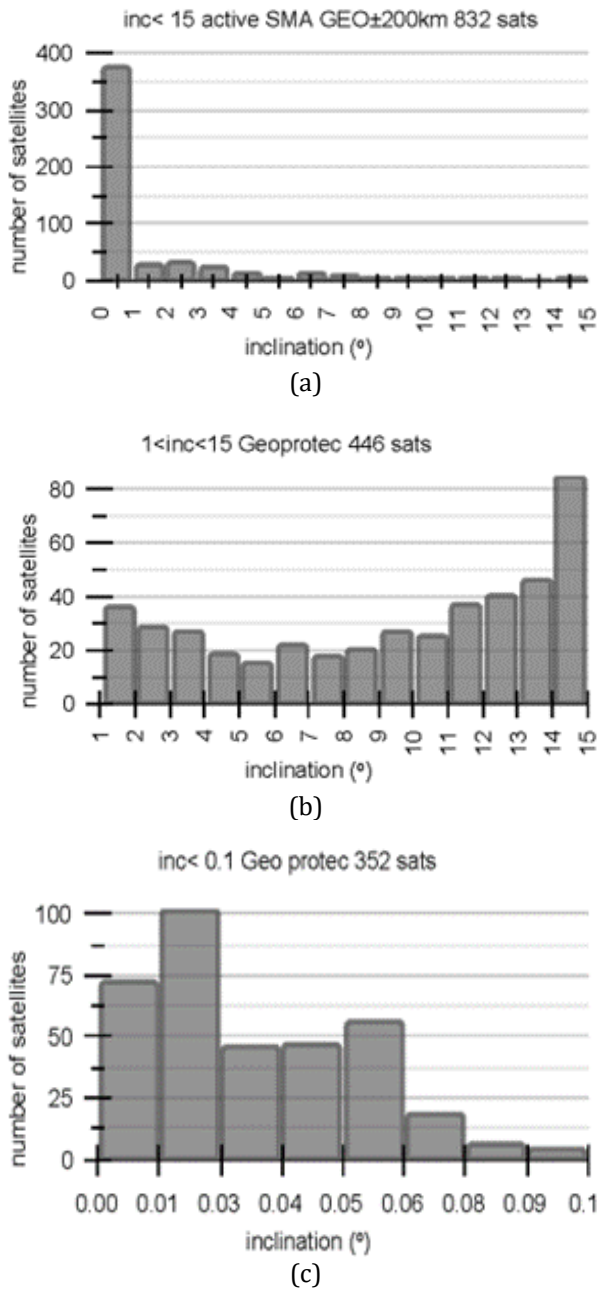


Figure 2. The number of satellites in geo and geo-protected region a) $i < 15^\circ$, b) $1^\circ < i < 15^\circ$, c) $i < 0.1^\circ$ (i.e., fully controlled and operational).

The bathtub curve is a common way to represent the failure rate of a satellite's component over time. The curve is shaped like a bathtub, with a high failure rate at the beginning (early life failures), a low failure rate in the middle (random failures), and a high failure rate again at the end (wear-out failures). Early life failures often occur just after the satellite is launched, but these can be eliminated through design and production improvements. The wear-out failures occur at the end of the equipment's life and can be delayed through proper design and production methods. The random failure period is where the failure rate is low and stable and is generally considered the equipment's practical life.

These failures are primarily due to factors such as working conditions and external environmental conditions causing equipment stress to exceed a certain level [6].

The space environment can cause various types of damage to the satellite, such as radiation damage, micrometeoroid impact, and thermal stress. In addition, the initial design, manufacturing, and assembly quality can affect the equipment's performance.

Geostationary satellites, like any complex system, can fail for various reasons and may not be able to move them to the graveyard region. Some common causes of geostationary satellite failure include power systems, propulsion systems, structural electronic equipment, and software failures. Geostationary satellites are exposed to a harsh space environment, which can cause damage over time. Solar radiation, cosmic radiation, and temperature extremes can all contribute to satellite failure [7, 8].

The malfunction of a geostationary satellite can result in significant consequences, depending on the purpose and services of the satellite. The malfunctioning satellites can not maneuver and revolve under natural forces. The impact of natural forces in space can alter the satellite's orbit, and the satellite may remain in the geostationary region, the protected geostationary region, or the graveyard region.

2. Geo satellite natural motion

The orbital behavior of a geostationary satellite is influenced by multiple factors, such as the gravitational attraction of the Earth, the solar wind, and the gravitational forces exerted by other celestial bodies.

Table 1 provides the perturbations acting on a geosynchronous satellite that can cause the satellite's orbital elements to vary over time. These variations are categorized into three main groups: short-periodic (SP), long-periodic (LP), and secular (SC) terms. Short-periodic perturbations affect parameters like the semi-major axis, eccentricity, inclination, ascending node, and argument of perigee, attributable to factors such as Earth's non-spherical mass distribution, gravitational forces from the Moon and the Sun, and solar radiation pressure. These changes occur at shorter intervals, spanning days or months. Long-periodic variations also impact the same orbital elements but over longer durations, such as yearly or multi-year spans, due to influences like gravitational forces from the Moon and the Sun, as well as solar radiation pressure. These distinctions delineate the diverse timescales and influences behind alterations in satellite orbits [9, 10].

Secular variations affect the semi-major axis, eccentricity, inclination, ascending node, and argument of perigee. Perturbations cause these variations with no periodic component, resulting in a continuous change in the satellite's orbital elements over an extended period. These variations can be caused by factors such as solar radiation pressure, the moon's and sun's attraction, and the non-uniform mass distribution of the Earth, as shown in Table 1 [11].

The inclination and the rate of eccentricity growth play a role in computing the time spent in the GEO region.

One important factor affecting the long-term orbital behavior of a geostationary satellite is the Earth's gravitational attraction. The satellite's orbit is an ellipse (very close to a circle), with the Earth at one focus. Over time, the Earth's gravitational attraction causes the satellite's orbit to precess or slowly rotate around the Earth. This precession is caused by the fact that the Earth is not a perfect sphere and has a slightly oblate shape.

The solar wind, a stream of charged particles emanating from the Sun, can also affect the long-term

orbital behavior of a geostationary satellite. The solar wind can exert a small but measurable force on the satellite, causing its orbit to drift over time.

The gravitational attraction of other celestial bodies, such as the Sun and Moon, can also affect the long-term orbital behavior of a geostationary satellite. The gravitational attraction of these bodies can cause the satellite's orbit to become more or less elliptical over time [12 -16].

Table 1. The short-periodical term (SP), the long-periodical term (LP), and the secular term (SC) effect on a GEO satellite orbital elements.

Orbital elements	Solar radiation Pressure	Non-uniform mass distribution of Earth	Moon and Sun Attraction
Semi major axis	SP+LP	SP	SP+LP
Eccentricity	SP+LP	SP	SP+LP+SC ↑
Inclination (°)	SP+LP+SC ↑	SP	SP+LP+SC ↑
Right ascending node (°)	SP+LP+SC ↓	SP+SC ↓	SP+LP+SC ↓
Argument of perigee (°)	SP+LP	SP+SC ↑	SP+LP+SC ↓

2.1 Satellite dynamic model

Numerical methods for modeling the motion of satellites in orbit are snowballing as computer technology improves. This is because numerical methods have the advantage of being able to incorporate any perturbing force at any point during the simulation. This is achieved by adding the perturbing forces to the two-body equation, also known as Cowell's formulation. As a result, total acceleration of the satellite can be calculated as (Equation 1):

$$a = -\frac{\mu}{r_e}r + a_{perturbed} \tag{1}$$

$$U = \frac{\mu}{r} \left[1 + \sum_{l=2}^{\infty} \sum_{n=2}^l \left(\frac{R_e}{r}\right)^l P_{l,n} \sin\varphi_{sat} \{C_{l,n} \cos(n\lambda_{sat}) S C_{l,n} \sin(n\lambda_{sat})\} \right] \tag{2}$$

$$a_{gravity} = -\nabla U \tag{3}$$

The third body gravitational effect refers to the gravitational attraction exerted on a satellite by celestial bodies such as the Earth and the moon. Third-body gravitational effects can cause perturbations in a satellite's orbit, leading to changes in the satellite's orbital elements. The third body gravitational effect can be modeled using numerical methods and included in the calculation of a satellite's orbit. The GM 2008 and other recent gravity models take into account the third-body gravitational effect and use them to improve the accuracy of satellite orbit prediction. The acceleration caused by these bodies can be represented by Equation 4.

$$a_{3rd\ body} = \mu_{3rd} \left(\frac{r_{sat,3}}{r_{sat,3}^3} - \frac{r}{r^3} \right) \tag{4}$$

where, μ_{3rd} : gravitational parameters of moon and Sun, $r_{sat,3}$: vector from sat to 3rd body.

Solar radiation pressure is a force exerted on a satellite by the Sun's electromagnetic radiation. Solar

radiation pressure can affect a satellite's orbit by causing perturbations. The effect of solar radiation pressure on a satellite's orbit can be modeled using numerical methods and included in the calculation of the satellite's orbit. In addition to other forces, the model also considers the effect of solar radiation pressure described in Equation 5.

As the most significant force affecting a satellite in orbit, gravity is not uniform due to the Earth's irregular shape. Therefore, the gravitational force varies based on the satellite's position. A decomposition of spherical harmonics represents the gravitational potential (U) to account for the asymmetric distribution of the Earth, as outlined in the references [17, 18] (Equation 2-3).

where: λ : longitude of satellite, φ : geocentric satellite latitude, R_e : Earth mean radius, $P_{l(n)}$: Legendre polynomial, $C_{l(n)}$ and $S_{l(n)}$ gravitational coefficient from EGM2008 model, L and n : degree and order of decomposition.

$$a_{srp} = -v \frac{C_r A_s}{m} \frac{p_{sr}}{r_{sat,sun}^2} r_{sat,sun} \tag{5}$$

where; v : the shadow function 0 if sat in shadow; 1 otherwise, C_r solar radiation coefficient between 1 and 2, a_{srp} : cross-section area seen by Sun, p_{sr} : solar radiation pressure [19,20].

3. Elevated eccentricity method

The developed elevated eccentricity method refers to a strategy or technique used to modify the orbit of a satellite by increasing its eccentricity. In the context of

the GEO (geostationary orbit) region, the elevated eccentricity method involves intentionally raising the eccentricity of satellites in order to reduce their time spent in the geostationary and geostationary-protected regions. By increasing eccentricity, satellites spend less time in the regions of interest.

The proposed methodology emphasizes the controlled management of longitude (semi-major axis) and eccentricity during nominal east/west maneuvers. The scheduling of maneuver times is optimized to maximize eccentricity, wherein one maneuver cycle occurs at apogee, followed by the next cycle at perigee, strategically preserving longitude. Moreover, this approach allows for natural eccentricity increases, provided other parameters permit such adjustments.

The equation to calculate the delta-v required to transition a satellite from GEO to a graveyard orbit is represented by Equation 6 [21].

$$\Delta v = 0.0336 * h_o \tag{6}$$

where, h_o denotes the raised orbit height in km, and ΔV signifies the increased delta-V in m/s.

When considering scenarios involving increases in perigee and apogee while maintaining the same semi-major axis, the simplified approximation remains valid.

However, this assumption assumes no additional delta-v is allocated to modify apogee and perigee independently. Instead, the delta-v from east-west maneuvers is utilized for both purposes, including natural eccentricity increases.

In this study, we consider the scenario where a satellite is rendered non-functional due to subsystem failure, fuel depletion, or other reasons, and it lacks the capability to maneuver to the graveyard orbit using its propulsion system.

The disposal of satellites with high eccentricity will still cross the GEO region. However, they may not cross the GEO population ring, which decreases the chance of collision compared to a scenario where the GEO population is evenly spread across the GEO region. The effectiveness of this method can be verified by calculating the amount of time the discarded satellite spends within the GEO-protected region ($GEO \pm 200$ km and inclination 15°).

This study employed six geostationary satellites with specific initial parameters (Sat0 to Sat5) for testing purposes, as shown in Table 2. The satellites were chosen with increasing eccentricity values, with Sat0 having the lowest and Sat5 having the highest. All the satellites were chosen with an inclination of 3° , an area-to-mass ratio of $0.02 \text{ m}^2/\text{kg}$, and an epoch date of January 1st, 2021, at 00:00:00 in the J2000 reference frame.

Table 2. Geostationary test satellites with different eccentricities.

Satellite	SMA (km)	Symbol	Eccentricity	Apogee (km)	Perigee (km)	ΔV (m/S)
Sat0	42166.300	e0	5.00×10^{-5}	35790.264	35786.048	0.00
Sat1	42166.300	e1	1.78×10^{-3}	35863.157	35713.155	0.15
Sat2	42166.300	e2	4.74×10^{-3}	35988.157	35588.155	1.83
Sat3	42166.300	e3	8.30×10^{-3}	36138.158	35438.154	5.46
Sat4	42166.300	e4	1.19×10^{-2}	36288.160	35288.152	10.89
Sat5	42166.300	e5	3.00×10^{-2}	37053.165	34523.147	35.82

This data provides information about the orbital parameters of six satellites (Sat0-Sat5), including their semi-major axis (SMA) in kilometers, eccentricity symbol, eccentricity, apogee, and perigee altitude in kilometers. The semi-major axis for all the satellites is 42166.3 km, the average distance from the Earth's center to the satellite. The eccentricity symbol (e0-e5) denotes the different levels of eccentricity for each satellite. Eccentricity measures how much the orbit deviates from a perfect circle. The apogee and perigee are the highest and lowest points of the orbit, respectively. The data shows that as the eccentricity increases, the apogee and perigee altitudes increase, and the difference between apogee and perigee altitudes increases. The final column in Table 2 furnishes the requisite delta-v (dV) needed to attain the specified eccentricity value from the initial e0 scenario. Notably, while the table indicates the dV required, executing maneuvers solely to alter eccentricity values is not advised. The expected approach involves augmenting eccentricity during longitude-keeping maneuvers.

Determining a satellite's orbit relies on observational data from ground-based or space-based systems. These systems collect observed and measured datasets, which serve as crucial inputs for orbit estimation. Global Navigation Satellite Systems (GNSS), designed initially to

furnish precise positioning and timing information for both military and civilian users [22-25], have emerged as a primary tool for Precise Point Positioning (PPP) and diverse civil applications [25]. Integrating spaceborne GNSS receivers onto geosynchronous communication satellites presents an efficacious alternative for orbit determination compared to conventional methods [26]. Utilizing observation data obtained from GNSS or ground tracking systems, we implement the High-Performance Orbit Propagator (HPOP). This numerical propagation method employs a specific type of numerical integration known as the Runge-Kutta-Fehlberg method of order 7-8. The HPOP serves as a robust technique for satellite orbit determination, facilitating precise and efficient calculations essential for space missions [27].

The theoretical altitude of the satellites over a period of two days is shown in Figure 3a. The figure illustrates the boundary of the geostationary-protected region with a dashed red line and the boundary of the geostationary region with a green line. It can be observed from the figure that the altitude of the satellite's changes with time and with the eccentricity of the satellite. Figure 3b illustrates the intersection of the geostationary region and the actual satellite orbit in the X-Y plane. Minimizing this intersection line will decrease the time the satellite spends in the geostationary region. The satellite's orbit is

analyzed over various time periods, including 1 day, 8 years, and 140 years. The short-term and long-term behavior of the satellite in this orbit is evaluated by monitoring its time spent in the geostationary and geostationary-protected regions.

In this study, the satellites with orbital parameters provided in Table 2 were used to calculate the time spent

in the geostationary region. The orbital data was propagated using the high orbit propagating (HPOP) method described in section 2.1. The HPOP method is known for its high accuracy in determining the orbital behavior of a satellite, and thus the time spent in the geostationary region was obtained with high precision.

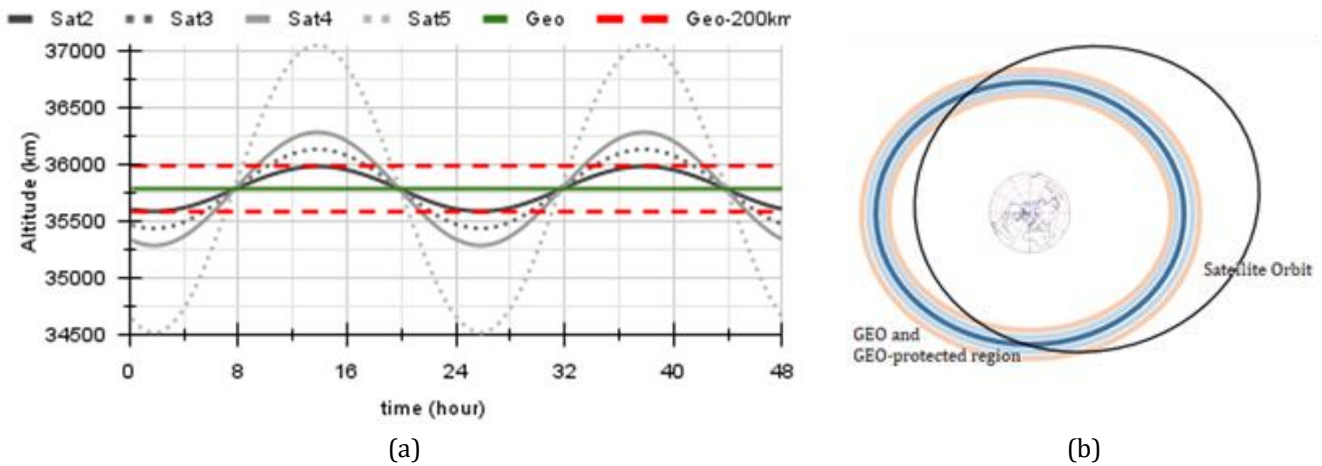


Figure 3. a) Sat2 to Sat5 altitude variation for two days. **b)** GEO, GEO-protected, and moderate eccentricity satellite orbits viewed from the north (not to scale).

A satellite operator typically requires approximately 12 m/s of ΔV to reposition a GEO satellite 350 km above the designated GEO region. This maneuver is theoretically executed as two equal maneuvers, separated by 12 hours, when the satellite is at its apogee. In practical applications, this operation is often divided into 4 or even 8 separate maneuvers as per industry practices.

In scenarios where no failures occur, these repositioning operations are conducted in accordance with established procedures. However, when a failure occurs and the satellite cannot be appropriately repositioned, a satellite with zero eccentricity would spend a significant portion of its time within the GEO region. In contrast, in an elevated eccentricity scenario, should the same issue arise, the residence time of the aging satellite in the GEO region would be significantly reduced.

When a geostationary satellite malfunctions for any reason, it is subject to natural forces that cause it to change in its orbit. Analyzing the satellite's orbital

parameters, such as eccentricity, longitude, and semi-major axis in natural cases, makes it possible to estimate how long the satellite will remain in the geostationary or geostationary-protected region. Minimizing the time spent in the geostationary region can help reduce the accumulation of debris in that area.

4. Results and Discussion

This paper introduces a novel strategy to safeguard both the geostationary and geostationary-protected regions by implementing elevated eccentric operations for aging satellites in case of orbit raising failure.

The altitude of satellites varies over time due to their orbital parameters. Eccentricity plays a significant role in the variation of altitude. Figure 4a illustrates the distance of three selected sample satellites, Sat1, Sat3, and Sat5, from the GEO zero orbit (35786 km). Figure 4b displays the time spent in the GEO region for Sat0 to Sat5. The graph shows that satellites with high eccentricity have a greater distance to the GEO zero orbit and spend less time in the GEO region.

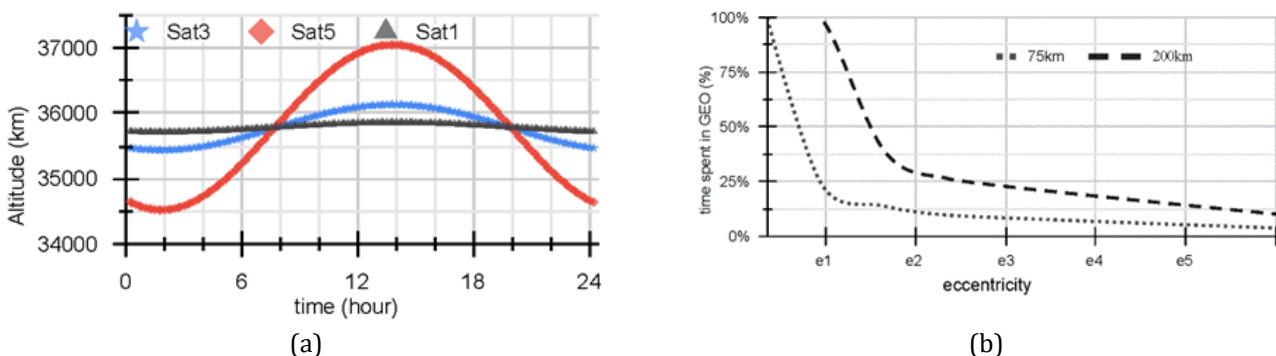


Figure 4. a) Sat1, Sat3, and Sat5 orbit distance to GEO for 24 hours **b)** satellite spent time in GEO and GEO protected region for eccentricity e0 to e5.

Table 3 provides information about the time spent in the regions of interest (from 75 km to 500 km) for each satellite without orbit perturbation. Sat4 and Sat5 spend 73.81% and 89.89% of one revolution's time in the graveyard region, while Sat1, Sat2, and Sat3 do not reach the graveyard region. As the eccentricity of a satellite increases, the time spent in the geostationary region decreases, which helps to mitigate the amount of time

spent in the geostationary and geostationary protected regions.

With this method, by increasing the eccentricity to a value of $e=0.03$, as shown in Table 3, it is estimated that a satellite would spend only 3.77% of its orbital revolution in the geostationary region, 6.33% in the geostationary protected region and the majority in the super-geostationary (graveyard) region.

Table 3. Sat0 to Sat 5 time spent in GEO, GEO protected and graveyard region.

Sat	0-75km	75-200km	200-350km	350-500km	500+ km	ecc	ecc
Sat0	100.00%	0.00%	0.00%	0.00%	0.00%	5.00×10^{-5}	e0
Sat1	99.76%	0.24%	0.00%	0.00%	0.00%	1.78×10^{-3}	e1
Sat2	24.47%	75.29%	0.24%	0.00%	0.00%	4.74×10^{-3}	e2
Sat3	13.75%	24.97%	61.04%	0.24%	0.00%	8.30×10^{-3}	e3
Sat4	9.58%	16.61%	23.17%	50.40%	0.24%	1.19×10^{-2}	e4
Sat5	3.77%	6.33%	7.74%	8.02%	74.13%	3.00×10^{-2}	e5

Figure 5 provides the results of Sat0 to Sat5's time spent in the GEO, GEO protected, and graveyard regions and shows the time spent in each region. An increase in eccentricity results in the satellite spending more time at higher altitudes, which reduces the time spent in the GEO region.

Figure 5, x-axis provides information about the time spent by the satellites in different altitude regions, and

the y-axis shows the eccentricity values of Sat0 to Sat5.

The impact of natural forces on the orbital behavior of satellites over the medium and long term was analyzed in terms of the time spent in the GEO and GEO protected region. Figure 6a and 6b depict the effect of operating an aging satellite with moderate eccentricity on the changes in eccentricity and the altitude of apogee and perigee over an 8 and 15-year period in the GEO region.

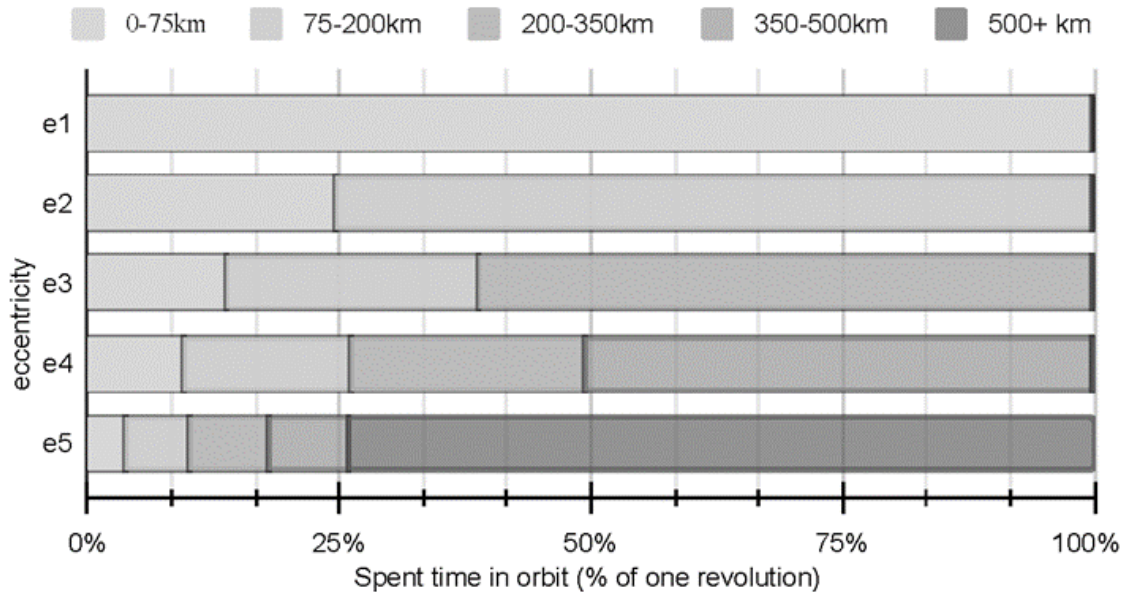


Figure 5. Percentage of time spent in a different region for Sat0 to Sat5.

Figure 6a shows the fluctuation of eccentricity between 1.1×10^{-5} and 8.05×10^{-4} . Figure 6b) displays the long-term changes in the apogee and perigee altitude, ranging between 35947.088 km and 35833.585 km for apogee and between 35737.402 km, and 35790 km for perigee. In Figure 6b, the x-axis represents the time in years, and the y-axis displays the varying orbital parameters of the satellite.

Figure 6c, the changes in longitude over an 8-year period, with the maximum value reaching 122.565° and the minimum value being 24.789° . Figure 6d demonstrates the right ascension of the ascending node

(RAAN), which has a period of around 52 years, and RAAN varies between 0 and 360° for 140 years.

Figure 7a and 7b demonstrate the impact of operating the aging satellite Sat1, with a moderate eccentricity, on the variation of the satellite's eccentricity and altitude of its apogee and perigee over 140 years in the geostationary region. Figure 7a shows the eccentricity variation, ranging from 7.1×10^{-5} to 1.465×10^{-3} . Figure 7b illustrates the long-term changes in the altitudes of the apogee and perigee, with a range of variation in apogee altitude from 35873.843 km to 35768.695 km and perigee altitude from 35807.058 km to 35707.759 km.

The x-axis represents time in years, the left y-axis in blue shows the altitude of apogee variation, and the right y-axis in red shows the altitude of perigee variation in km.

The semi-major axis, the argument of perigee, the right ascension of the ascending node, and the inclination orbital elements do not significantly affect the amount of

time spent in the GEO region. These elements have periods of 2.57, 1.07, and 52.5 years, respectively. Eccentricity, however, significantly impacts the time spent in GEO, as an increase in eccentricity results in a decrease in the amount of time spent in the region for all satellites.

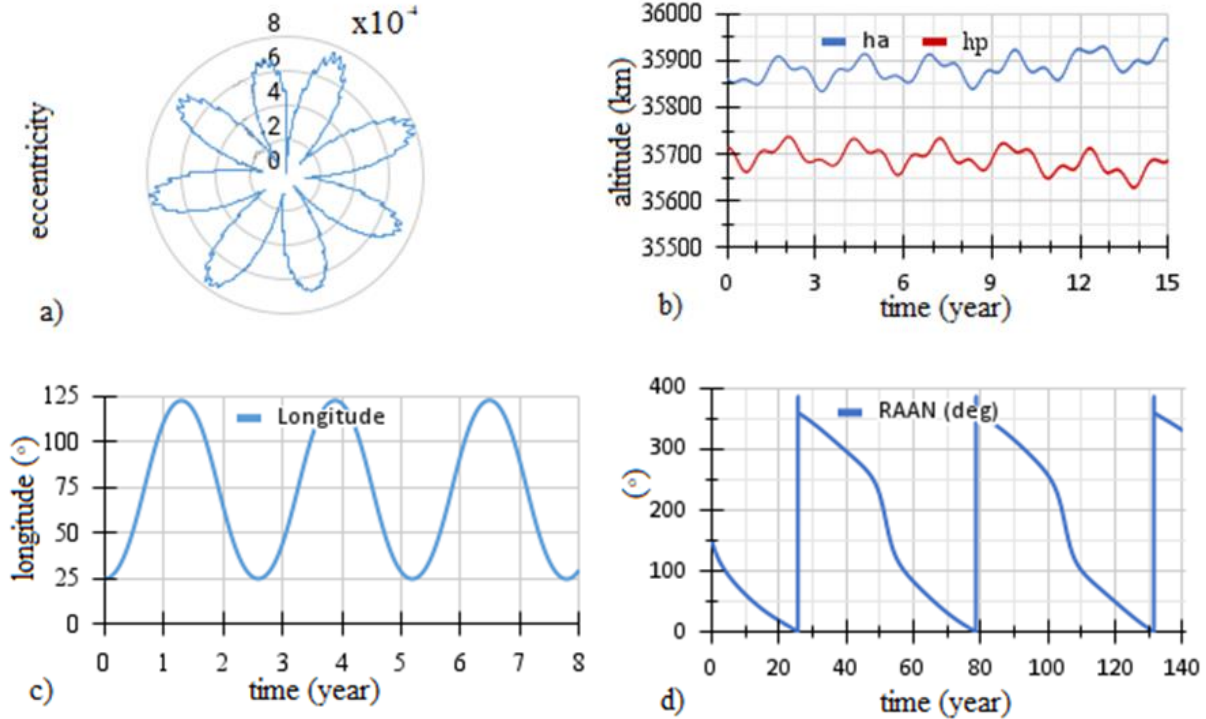


Figure 6. a) Eccentricity variation of Sa0 for 8 years, b) Altitude of apogee and perigee variation over 15 years, c) Longitude change for 8 years, d) Right ascension of ascending node over 140 years.

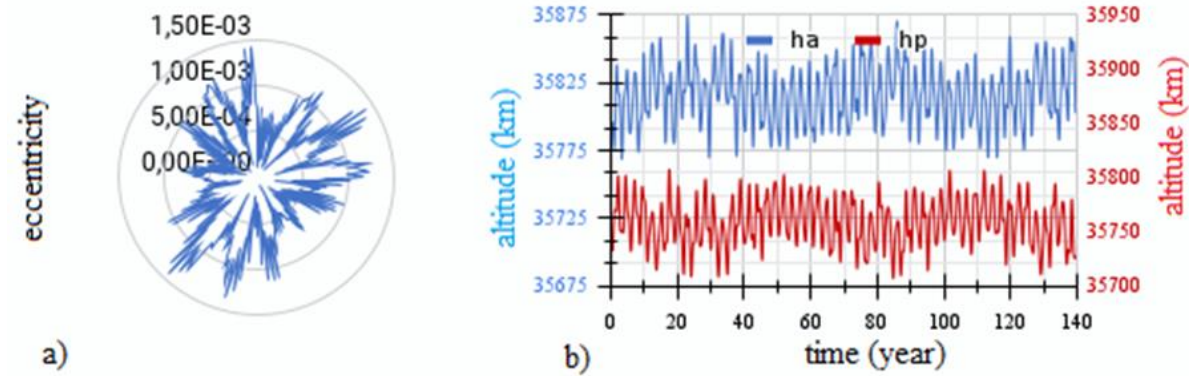


Figure 7. a) Eccentricity variation and b) Altitude of apogee and perigee variation over 140 years for Sat1.

Sat0 and Sat5 have been selected as representative samples of all satellites to give a comprehensive overview of the variations in orbital elements. Sat0 has a low eccentricity, while Sat5 has a high eccentricity. Table 4 displays the changes in the orbital parameters of Sat0 and Sat5 over time, with each row representing a different orbital element. The columns depict the statistical values for each orbital parameter. The table highlights the effect of natural forces on the orbital parameters over time, such as Earth's gravity, solar radiation pressure, and other third-body gravitational effects.

Table 4 compares the orbital elements of two satellites, Sat0 and Sat5. The semi-major axis (SMA) of

both satellites is very similar. The inclination of Sat0 has a range of 15.0° to 0.0° , with a standard deviation of 5° and a difference of 15.0° . Sat5 has similar values, ranging from 15.0° to 0.0° , with a standard deviation of 5° and a difference of 15.0° . The right ascension of the ascending node and the argument of perigee of both satellites are similar. The longitude of both satellites has changed slightly, but the difference is not significant.

The eccentricity of Sat0 is 5×10^{-5} , which is constant, while that of Sat5 is 0.03° with a standard deviation of 0 and a delta of 0.01° . This indicates that Sat5 has a small elliptical orbit. Regarding altitude, the apogee for Sat0 has a maximum value of 35878.89 km, a minimum of 35761.64 km, a standard deviation of 22.48 km, and a

delta of 117.25 km. The same parameters for Sat5 are 37245.98 km, 36983.65 km, 48.82 km, and 262.34 km. The perigee altitude for Sat0 has a maximum value of 35814.28 km, a minimum of 35701.77 km, a standard deviation of 22.64 km, and a delta of 112.51 km. The same parameters for Sat5 are 34585.16 km, 34328.68

km, 48.43 km, and 256.48 km. Finally, the difference in apogee and perigee altitude for Sat0 is 129.63 km with a standard deviation of 26.81 km and a delta of 128.02 km. For Sat5, these values are 2870.61 km, 2444.98 km, 90.25 km, and 425.63 km, respectively.

Table 4. Orbital elements evolution under the natural forces (perturbed orbit) over 140 years for Sat0 and Sat5.

Orbital Elements	Sat0 max	Sat0 min	Sat0-stddev	Sat0 delta - max-min	Sat5 max	Sat5 min	Sat5 stddev	Sat5 delta - max-min
SMA (km)	42193.35	42138.04	18.15	55.31	42193.30	42138.10	18.11	55.20
ecc	0.00	0.00	0.00	0.00	0.03	0.03	0.00	0.01
Inc (°)	15.00	0.00	5.00	15.00	15.00	0.00	5.00	15.00
RAAN (°)	359.99	0.03	128.91	359.96	359.97	0.01	129.00	359.96
Aop (°)	359.91	0.03	102.52	359.88	359.97	0.03	101.60	359.94
Ha (km)	35878.89	35761.64	22.48	117.25	37245.98	36983.65	48.82	262.34
Hp (km)	35814.28	35701.77	22.64	112.51	34585.16	34328.68	48.43	256.48
deltaAP (km)	129.63	1.60	26.81	128.02	2.870.61	2.444.98	90.25	425.63
Longitude (°)	123.39	24.53	35.43	98.86	123.40	24.43	35.42	98.97

The study also found that changes in the semi-major axis and eccentricity can affect a satellite's apogee and perigee, influencing the time spent in the geostationary region. By analyzing the orbital behavior of the satellite under natural forces, the time spent in the geostationary region was calculated, providing insights into strategies for mitigating space debris. Overall, the comparison shows that Sat0 and Sat5 have similar orbital elements but with some differences, especially in terms of eccentricity and altitude. The differences in eccentricity change the spent time in GEO and GEO-protected regions.

Table 5 presents information about six satellites, Sat0 to Sat5, with varying eccentricity values. Sat0 has an eccentricity of 5×10^{-5} , while Sat1, Sat2, Sat3, Sat4, and Sat5 have eccentricity values of 1.77×10^{-3} , 4.74×10^{-3} , 1.18×10^{-2} , and 3×10^{-2} , respectively. Sat1 and Sat2 spend

all of their time in the geostationary region for one revolution, while Sat3, Sat4, and Sat5 spend 25.0%, 13.85%, 9.72%, and 3.47% of 1 revolution's time in the geostationary region. Similarly, Sat0, Sat1, and Sat2 spend all of their time in the geostationary protected region, but Sat3, Sat4, and Sat5 spend 39.58%, 26.39%, and 9.73% of one revolution's time in the geostationary protected region.

Table 5 also displays the medium and long-term fluctuations in the amount of time satellites spend in GEO and its protected region. The data reveals that the variations are around 0.4% to 0.5%, which are relatively small and suggest that medium and long-term changes in orbital parameters have a limited effect on the time spent in the GEO region.

Table 5. Geo satellites spent time around the GEO region for short, medium, and long term.

Time	Region Boundary	Sat0 (%)	Sat1 (%)	Sat2 (%)	Sat3 (%)	Sat4 (%)	Sat5 (%)
8 years	GEO±75 km	100.0	75.79	24.20	13.70	9.61	3.81
	GEO±200 km	100.00	100.00	85.97	38.63	26.24	10.18
1 year	GEO±75 km	100.00	75.68	24.16	13.64	9.61	3.82
	GEO±200 km	100.00	100.00	85.42	38.54	26.15	10.14
1 day	GEO±75 km	100.00	100.00	25.00	13.89	9.72	3.47
	GEO±200 km	100.00	100.00	100.00	39.58	26.39	9.72

Figure 8 shows Sat0 to Sat5 spent time in GEO and GEO-protected regions to analyze the effect of short, medium, and long duration in the GEO region. Figure 8 shows the percentage of time that given satellites, identified by the "e" values (e0, e1, e2, etc.) time spent in different regions over a specified time period. The first column, "8Y:G" indicates 8 years in the "GEO" region, while "8Y:GP" indicates 8 years in the "GEO protected" region. The other columns, "1Y:G", "1Y:GP", "1D:G", "1D:GP" indicate 1 year and 1 day in the GEO and GEO-protected regions, respectively. The percentage values in each cell of the table indicate the percentage of time that the respective satellite spent in the corresponding region over the specified time period. The trend line shown in black describes the path that the data points in Figure 8

converge to zero as e increases. It implies that high eccentricity decreases time spent in the GEO region.

With this method, by increasing the eccentricity to a value of $e=0.03$, it is obtained that a satellite would spend less time in the geostationary and the geostationary protected region; it can be shown clearly from the graph that as eccentricity increases, the time spent in GEO and GEO protected regions decreases. Therefore, operating aging satellites with moderate eccentricity can be an effective method to empty the GEO region. By increasing the eccentricity of a satellite, it is possible to reduce the amount of time it spends in the geostationary region and thus reduce the risk of collisions and the amount of debris in that region. Additionally, by analyzing the orbital behavior of the satellite, it is possible to ensure

the long-term sustainability of the GEO region and mitigate space debris.

The utilization of the elevated eccentricity method by an operator is suggested to potentially reduce the

duration in the GEO and GEO-protected regions in the event of an orbit-raising failure. However, a successful orbit-raising operation may render the use of the elevated eccentricity method unnecessary.

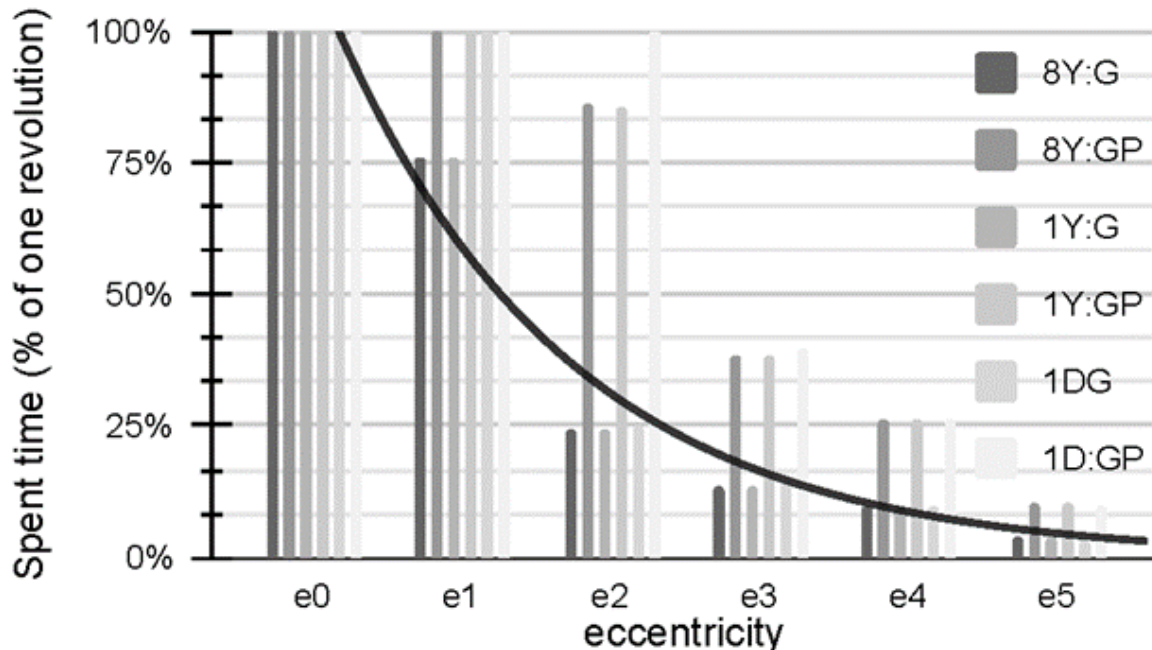


Figure 8. Short, medium and long-term satellites that is under the natural forces (perturbed orbit) spent-time in GEO and GEO protected region evolution and eccentricity trend line.

Many efforts can be made to decrease the time the satellite spends, thereby carefully controlling its initial orbital parameters, such as eccentricity, to mitigate the buildup of space debris. Moreover, employing innovative methods as a backup solution for operating aging satellites can significantly reduce the risk of space debris accumulation. This strategic approach is critical in the sustainability of space operations for all satellite operators.

5. Conclusion

This study shows that operating aging satellites with high eccentricity can effectively mitigate the risk of space debris. As eccentricity increases, the time a satellite spends in the geostationary region decreases, reducing the risk of collisions and the amount of debris in that region. The study found that the time the satellite spent in the geostationary region stayed consistently low over 140 years, confirming this method's effectiveness. This method may not be needed if the satellite's orbit-raising operation is successful. It is advantageous in the case of partially successful orbit raising.

In conclusion, operating aging satellites with elevated eccentricity effectively mitigate space debris by reducing time spent in the geostationary region. This method is relatively simple and inexpensive. While the elevated eccentricity method effectively protects GEO from debris, it should be used with other long-term sustainability techniques.

Conflicts of interest

The authors declare no conflicts of interest.

References

1. Delong, N., & Frémeaux, C. (2005). Eccentricity management for geostationary satellites during end of life operations. In 4th European Conference on Space Debris, 587, 297. Darmstadt: ESA Special Publication.
2. Xu, W., Liang, B., Li, B., & Xu, Y. (2011). A universal on-orbit servicing system used in the geostationary orbit. *Advances in Space Research*, 48(1), 95-119. <https://doi.org/10.1016/j.asr.2011.02.012>
3. Johnson, N. L. (2012). A new look at the GEO and near-GEO regimes: Operations, disposals, and debris. *Acta Astronautica*, 80, 82-88. <https://doi.org/10.1016/j.actaastro.2012.05.024>
4. Öz, İ., & Yılmaz, Ü. C. (2020). Determination of coverage oscillation for inclined communication satellite. *Sakarya University Journal of Science*, 24(5), 973-983. <https://doi.org/10.16984/saufenbilder.702190>
5. Oz, I. (2022). Salınlı yörünge haberleşme uydularında 2 eksen düzeltmeli kapsama alanı stabilizasyonu. *Journal of The Faculty of Engineering and Architecture of Gazi University*, 38(1), 219-229. <https://doi.org/10.17341/gazimmfd.960480>
6. Fu, S. Y., Wang, Z. R., Shi, H. L., & Ma, L. H. (2018, June). The application of decommissioned GEO satellites to CAPS. In *IOP Conference Series: Materials Science and Engineering*, 372(1), 012033. <https://doi.org/10.1088/1757-899X/372/1/012033>
7. Tafazoli, M. (2009). A study of on-orbit spacecraft failures. *Acta Astronautica*, 64(2-3), 195-205. <https://doi.org/10.1016/j.actaastro.2008.07.019>

8. Cougnet, C., Gerber, B., Heemskerk, C., Kapellos, K., & Visentin, G. (2006). On-orbit servicing system of a GEO satellite fleet. In 9th ESA Workshop on Advanced Space Technologies for Robotics and Automation 'ASTRA.
9. Dong, X., Hu, C., Long, T., & Li, Y. (2016). Numerical analysis of orbital perturbation effects on inclined geosynchronous SAR. *Sensors*, 16(9), 1420. <https://doi.org/10.3390/s16091420>
10. Anselmo, L. (2004). The long-term evolution of the Italian satellites in the GEO region and their possible interaction with the orbital debris environment. In 54th International Astronautical Congress of the International Astronautical Federation, the International Academy of Astronautics, and the International Institute of Space Law, IAC-03-IAA.5.2.05. <https://doi.org/10.2514/6.IAC-03-IAA.5.2.05>
11. Rosengren, A. J., Scheeres, D. J., & McMahon, J. W. (2013). Long-term dynamics and stability of GEO orbits: the primacy of the Laplace plane. In Proceedings of the AAS/AIAA Astrodynamics Specialist Conference, Hilton Head, South Carolina, AAS 13-865.
12. Jenkin, A. B., McVey, J. P., & Sorge, M. E. (2022). Assessment of time spent in the LEO, GEO, and semi-synchronous zones by spacecraft on long-term reentering disposal orbits. *Acta Astronautica*, 193, 579-594. <https://doi.org/10.1016/j.actaastro.2021.07.048>
13. Mei, H., Damaren, C. J., & Zhan, X. (2021). End-of-life geostationary satellite removal using realistic flat solar sails. *Aerospace Systems*, 4, 227-238. <https://doi.org/10.1007/s42401-021-00089-8>
14. Cabrières, B., Alby, F., & Cazaux, C. (2012). Satellite end of life constraints: Technical and organizational solutions. *Acta Astronautica*, 73, 212-220. <https://doi.org/10.1016/j.actaastro.2011.10.014>
15. Yilmaz, N. (2023). Assessment of latest global gravity field models by GNSS/Levelling Geoid. *International Journal of Engineering and Geosciences*, 8(2), 111-118. <https://doi.org/10.26833/ijeg.1070042>
16. Yilmaz, M., Turgut, B., Gullu, M., & Yilmaz, I. (2016). Evaluation of recent global geopotential models by GNSS/Levelling data: internal Aegean region. *International Journal of Engineering and Geosciences*, 1(1), 18-23. <https://doi.org/10.26833/ijeg.285221>
17. Vallado, D. A. (2001). *Fundamentals of astrodynamics and applications*, 12. Springer Science & Business Media.
18. Montenbruck, O., Gill, E., & Lutze, F. (2002). *Satellite orbits: models, methods, and applications*. *Applied Mechanics Reviews*, 55(2), B27-B28. <https://doi.org/10.1115/1.1451162>
19. Öz, İ. (2024). Eş konumlu uyduların yaklaşma izlenmesine gerçek zamanlı mesafe ölçümü tabanlı yaklaşım. *Gazi Üniversitesi Mühendislik Mimarlık Fakültesi Dergisi*, 39(2), 825-834. <https://doi.org/10.17341/gazimmfd.1181262>
20. Atiz, Ö. F., Konukseven, C., Ögütçü, S., & Alcay, S. (2022). Comparative analysis of the performance of Multi-GNSS RTK: A case study in Turkey. *International Journal of Engineering and Geosciences*, 7(1), 67-80. <https://doi.org/10.26833/ijeg.878236>
21. Anselmo, L., & Pardini, C. (2017). On the end-of-life disposal of spacecraft and orbital stages operating in inclined geosynchronous orbits. In Proceedings of the 9th IAASS Conference, Session 05: Space Debris-I, 87-94.
22. Uçarlı, A. C., Demir, F., Erol, S., & Alkan, R. M. (2021). Farklı GNSS uydu sistemlerinin hassas nokta konumlama (PPP) tekniğinin performansına etkisinin incelenmesi. *Geomatik*, 6(3), 247-258. <https://doi.org/10.29128/geomatik.779420>
23. Pirtı, A., Gündoğan, Z. Ö., & Şimşek, M. (2022). QZSS uyduları ve sinyal yapıları. *Geomatik*, 7(3), 243-252. <https://doi.org/10.29128/geomatik.979823>
24. Pirtı, A., Hoşbaş, R. G., Şenel, B., Köroğlu, M., & Bilim, S. (2021). Galileo uydu sistemi ve sinyal yapısı. *Geomatik*, 6(3), 207-216. <https://doi.org/10.29128/geomatik.750469>
25. Altuntaş, C., & Tunaliolu, N. (2022). Retrieving the SNR metrics with different antenna configurations for GNSS-IR. *Turkish Journal of Engineering*, 6(1), 87-94. <https://doi.org/10.31127/tuje.870620>
26. Koca, B., & Ceylan, A. (2018). Uydu konum belirleme sistemlerindeki (GNSS) güncel durum ve son gelişmeler. *Geomatik*, 3(1), 63-73. <https://doi.org/10.29128/geomatik.348331>
27. Refaat, A., Badawy, A., Ashry, M., & Omar, A. (2018). High accuracy spacecraft orbit propagator validation. In The International Conference on Applied Mechanics and Mechanical Engineering, 18th International Conference on Applied Mechanics and Mechanical Engineering, 1-9. Military Technical College.

